Accepted Manuscript

Pin-on-disc investigation on copper-free friction materials dry sliding against cast iron

Mara Leonardi, Cinzia Menapace, Vlastimil Matějka, Stefano Gialanella, Giovanni Straffelini

PII: S0301-679X(17)30502-9

DOI: 10.1016/j.triboint.2017.10.037

Reference: JTRI 4938

To appear in: *Tribology International*

Received Date: 19 July 2017

Revised Date: 25 October 2017

Accepted Date: 27 October 2017

Please cite this article as: Leonardi M, Menapace C, Matějka V, Gialanella S, Straffelini G, Pin-on-disc investigation on copper-free friction materials dry sliding against cast iron, *Tribology International* (2017), doi: 10.1016/j.triboint.2017.10.037.

PIN-ON-DISC INVESTIGATION ON COPPER-FREE FRICTION MATERIALS DRY SLIDING AGAINST CAST IRON

Mara Leonardi[a], Cinzia Menapace[a], Vlastimil Matějka [b], Stefano Gialanella[a], Giovanni Straffelini[a]

[a] Dept. of Industrial Engineering, University of Trento, Via Sommarive 9, Povo, Trento, Italy

[b] Brembo S.p.A., Stezzano, Bergamo, Italy

KEYWORDS

Dry sliding; Friction material; Brake materials; Friction layer

ABSTRACT

The role of metallic fibers, present in brake pad materials, have been investigated with particular attention to the formation of the friction layer. The aim of the research was to establish an effective approach for the development of less polluting copper-free friction materials. Starting from a reference material, two more compositions were prepared: one obtained just by removing copper; in another, the quota of the removed copper fibers was replaced by steel fibers. The samples were wear tested and the results compared with those obtained with the reference material.

The worn surfaces exhibit specific features, like cracks and compacted wear debris, that provide useful indications for interpreting the main wear phenomena and for a further development of novel friction materials.

1.INTRODUCTION

Friction materials used for brake pads are composites that may contain up to 30 different ingredients. These ingredients are usually classified according to four main classes: reinforcing fibers, friction additives, fillers and binders [1, 2].

The friction phenomena occurring during sliding at the interface between the pads and the brake disc are rather complex and difficult to model. The inhomogeneous composition of the pads results in a particular surface structure of the friction layer forming on their surface as a consequence of the braking events. The friction layer is made up of primary and secondary plateaus. The reinforcements of the friction materials (hard particles and metal fibers), start protruding from the pad surface, as it starts wearing out, and form the “primary plateaus”. The primary plateaus are important for the growth of the secondary plateaus. These are made of wear debris blocked and compacted against the primary plateaus so to form continuous patches [3-5]. The shear and abrasive stresses generated by the sliding may damage secondary plateaus. Consequently, the life span of the disc-pad system features a dynamic equilibrium between the formation and disruption of the friction layer.

Copper is an important component of friction materials, and it is typically present in a composition range in between 1 and 15 wt.% [6]. Copper is added to the friction mixtures in the form of fibers and/or powders. Its primary role, as reported [7], is to increase the thermal conductivity of the brake pads, in order to reduce the contact temperatures at the pad-disc interface [8]. However, in a recent review [9], it has been emphasized that copper plays also other, is some respects, more important roles in the braking performances, considering that most of the heat generated by friction at the pad-disc interface is actually carried away by the disc and a small fraction only enters the pad [10]. Copper fibers form primary plateaus and therefore contribute to the formation of stable friction layers [11-14]. In addition, copper particles, coming from the powder fraction directly and from the wearing out of the fibers, become part of the secondary plateaus and favor their compaction [14-18]. In this way, smooth sliding conditions are achieved, with beneficial effects on the friction coefficient and noise reduction [18, 19]. Compact secondary plateaus are more resistant to wear damage and produce, on detachment, larger plate-like fragments, that are less prone to become airborne [20, 21].

Some recently published papers focused on the role of copper in promoting the formation of well compacted secondary plateaus, in which the metal is present as a fine nanometric dispersion, resulting from the comminution of the coarser components of the friction material during brake servicing. Considering this microstructural aspect, it has been proposed to add nano-grained copper particles directly to the pad mix, in order to render more efficient their embedding into the friction layer with the consequent possibility of using a relatively lower overall amount of copper [15, 22].

Alternatively, graphite particles, which are known to favor the compaction of the secondary plateaus by providing a velocity accommodation between the rotating disc and the sliding pads [23-25].

However, the legislation in the United States currently requires a reduction of copper in brakes to values below 5% by 2021 and 0.5% by 2025. These regulations have been implemented for the potentially toxic effects of copper-containing wear debris, once they are released into the environment [6, 26, 27]. In the European Union, no such limitations do exist at the present time on the use of copper in brake pads. Nonetheless, research efforts are being made to develop copper-free brake pads with adequate performances. Several brake companies are already manufacturing specific copper-free brake pads for the US and European market.

The present investigation is focused on the role of copper fibers in forming the primary plateaus and on the possibility of replacing them with steel fibers. In fact, steel fibers are reported to enhance the overall strength of the friction material [28], to form primary plateaus [29] and more uniform secondary plateaus, able to improve the friction and wear behavior of the material [30, 31]. However, a few investigations only can be found in the literature focusing on the specific role of steel and copper fibers on the wear mechanisms in brake pads. Quite often conflicting results are reported, which is quite unavoidable because of the complexity of the friction material compositions. There is a general agreement on the role of steel fibers in increasing the friction coefficient when sliding against cast iron rotors [32], with some controversy in the interpretation of these results. For example, Kumar and Bijwe [28] compared the friction and wear performances of different friction materials containing metallic fibers. It turned out that copper or brass fibers provide a better wear behavior than steel fibers. On the contrary, Park et al. [32] showed that a friction material containing 8% steel fiber has a better wear behavior than a similar steel-free material, containing 5% of copper. We started our investigation with reference to a copper-containing commercial friction material, already investigated in the past [15, 17, 21]. From this bench-mark, two novel friction materials were developed: the first was obtained by eliminating all of copper initially present in the original formulation. The second material was obtained by replacing all copper with steel fibers. The dry sliding behavior of the three materials was investigated using a pin-on-disc (PoD) test rig, followed by a careful characterization of the friction layers, using scanning electron microscopy (SEM), energy dispersive X-ray spectroscopy (EDXS) and image analysis.

2.EXPERIMENTAL PROCEDURES

2.1 MATERIALS

A commercial low-metallic friction material was used as a reference material. In the following it is referred to as Original Mix, *OM*. The main components (in wt%) of *OM* and their role are listed in Table 1. Copper is present both as fibers (~15 wt.%) and as powder in small amount (~1 wt.%). A copper-

free friction material was prepared by eliminating all copper from *OM*. This material is codenamed: *0Cu*. Another mixture, called *0Cu_Fe*, was prepared still eliminating all copper (fibers and powder) and by adding 15 wt.% of steel fibers to the *0Cu* sample. Thus, in this material, the copper fibers were replaced by steel fibers of the same kind already present in the *OM*. The designed formulations for the three materials tested in this work are listed in Table 2. The morphology of the steel fibers, as observed a SEM is shown in Fig. 1.

Constituents	**Main role**	**Amount, Wt%**
Steel (≈5%) Copper (≈15%)	Reinforcing fibers	20
Zirconia (≈22%), Potassium titanate, Graphite, Tin sulfide, Aluminium oxide	Friction additives	55
Vermiculite, Barite, Calcium carbonate	Fillers	15
Phenolic resin	Binder	10

Table 1. *Main constituents, their role and relevant concentrations in the Original Mix (OM) material.*

	OM	***0Cu***	***0Cu_Fe***
Original mix	100%	-	-
Original mix Cu free[a]	-	100%	85%
Steel fiber (addition)	-	-	15%
Density, g/cm^3	2.94	2.72	2.95
Hardness, Shore D	84	86	87

[a] *OM* without copper fibers and copper powder (~5 wt.% of steel fibers are already present).

Table 2. *Composition (wt%), designation and main properties of the friction materials under study.*

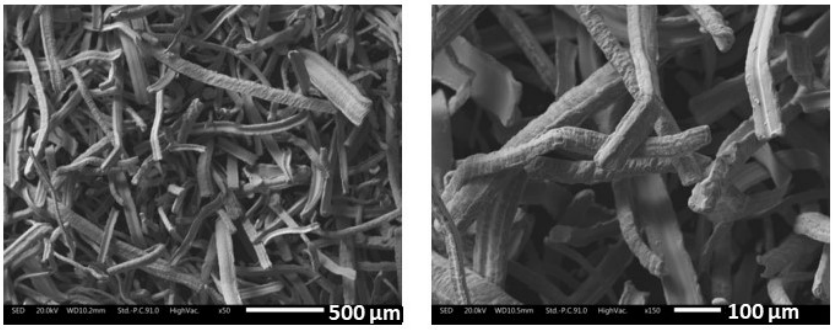

Fig.1 *SEM images at different magnifications of the steel fibers used for preparation of the mixture 0Cu_Fe.*

All the raw materials in the right concentrations were mixed up together using a Turbula shaker-mixer mill for 20 minutes. After homogenization, to prepare the pins for the wear testing, the right amount of each one of the powder mixtures was tap-pressed into a cylindrical mold of a hot-pressing apparatus, where stayed for 15 min at 150 °C and a pressure of 5 MPa. Successively, they were post-cured in an industrial oven for 10 h at 200 °C. At the end of the process, pins of 6 mm in diameter and 9 mm in height were obtained from each one of the three different mixtures (*OM*, *0Cu*, *0Cu_Fe*). The densities have been evaluated as the ratio of the pin mass and geometric volume. Relevant data are listed in Table 2. In this table, the experimental hardness values of the materials are also included. The disc used as counterface in the PoD tests was made of pearlitic grey cast iron with a hardness of 235 HV10.

2.2 WEAR TESTS

For reliable sliding tests, the pin surface must have a conformal contact with the disc. For this reason, the basal plane of each pin was grinded with a SiC 500 grit abrasive paper prior to starting the wear tests. The main parameters of the tests, performed at room temperature, were: sliding velocity of v=1.57 m/s and a nominal contact pressure of P_0=1 MPa. The testing parameters were selected on the basis of previous investigations and were aimed at obtaining mild sliding wear conditions [15, 17, 21, 33, 34]. The duration of each test was 7 hours, corresponding to a sliding distance of 39000 m. Specific tests were also stopped after 1 hour sliding, i.e., close to the end of the running-in stage, in order to obtain specific information on the surface damage evolution.

The friction coefficient was continuously recorded during the PoD tests. Two chrome-alumel thermocouples, placed in two holes drilled in the pin holder at a distance of 4.5 mm and 7.0 mm from the sliding surface, were used to record the pin temperature evolution during the tests. The mass of each pin was measured before and after the test with an analytical scale having a 10^{-4} g sensitivity. From the wear loss data, the wear volume, V (m^3), was calculated using the density values reported in Table 2. The wear of the pin was assessed by the specific wear coefficient (K_a):

$$K_a = V / F_n\, s$$

where V [m^3] is the measured wear volume, F_n [N] is the applied load and s [m] is the sliding distance [35]. The worn surface of the pins was observed with a scanning electron microscope, whereas the composition of the friction layer was measured by energy dispersive X-ray spectroscopy. The

extension of the primary and secondary plateaus was evaluated with image analysis carried out on SEM observations.

3.RESULTS

3.1 FRICTION AND WEAR

In Fig. 2 the evolution of the friction coefficients (μ) during the tests are shown. After a running-in stage with a duration of approximately 5000 s characterized by almost a continuous increase in the friction coefficient, a steady-state friction coefficient is attained. The mean values of the friction coefficient in the steady-state regime (μ_{ss}) are listed in Table 3. It can be also seen from Fig. 2 that the recording of the friction traces displays some scatter. The standard deviations of the steady-state friction coefficient, were evaluated. The relevant coefficient of variation (σ^*), defined as the ratio between the standard deviation and μ_{ss}, were calculated. The data obtained in this way are also included in Table 3. The *OM* shows the highest value of μ_{ss} and the smallest coefficient of variation, whereas the 0Cu material displays an opposite behavior. Eventually the *0Cu_Fe* material displays a behavior that is comparable to the *OM*.

Fig.3 shows the pin temperatures as a function of time. For the attainment of steady-state conditions, a sliding time of about 10000 s is required, which is longer than the time required for the friction coefficient to reach its steady state regime. The average steady-state temperatures, T_{ss}, are listed in Table 3. As expected, the T_{ss}-values correlate with the steady-state friction coefficients.

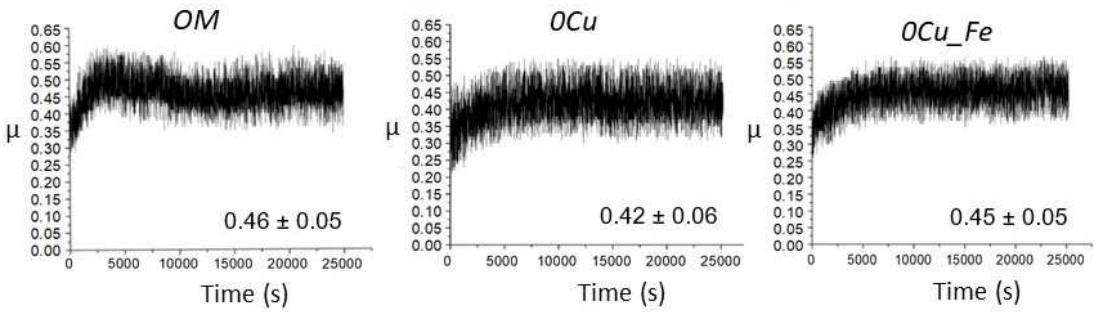

Fig.2 *Evolution of the friction coefficient (μ) for sample OM (a), 0Cu (b) and 0Cu_Fe (c), during pin-on-disc tests conducted for 7h. The steady state friction coefficients and relevant standard deviations for each material are indicated.*

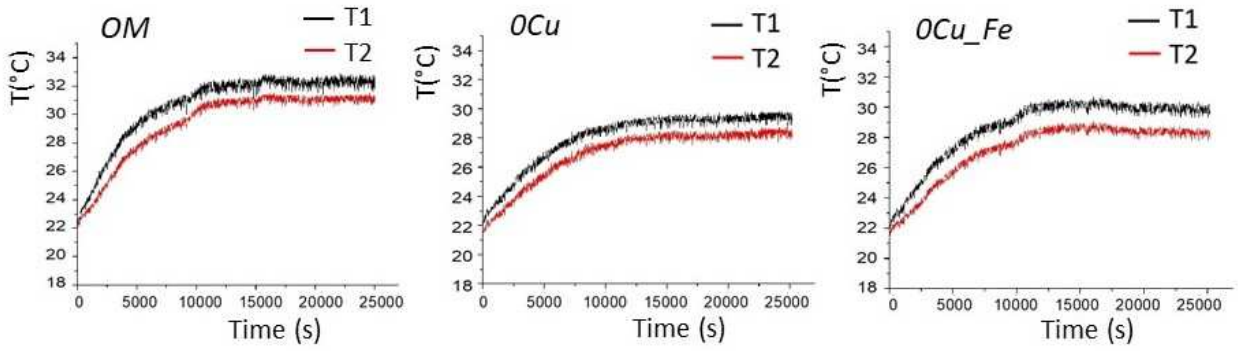

Fig.3 *Contact temperature as a function of time, measured by two thermocouples placed in two different parts of the pin, during pin-on-disc tests: OM, 0Cu, 0Cu_Fe.*

Material	**μ_{ss}**	**σ***	**T_{ss}, °C**	**K_a, m^2/N after 1 h**	**K_a, m^2/N after 7 h**	**η, %**
OM	0.46	0.11	33	$6.65*10^{-15}$	$3.34*10^{-15}$	- 50
0Cu	0.42	0.14	29	$6.91*10^{-15}$	$4.63*10^{-15}$	- 33
0Cu_Fe	0.45	0.11	30	$8.91*10^{-15}$	$4.02*10^{-15}$	- 55

Table 3 *Values of friction coefficient in the steady-state stage (μ_{ss}), coefficient of variation (σ*), steady-state temperatures (T_{ss}), specific wear coefficient (K_a) and percent variation of K_a (η) related to the samples OM, 0Cu and 0Cu_Fe resulting from PoD tests.*

As regards the wear data, the experimental specific wear coefficients (K_a) are included in Table 3. They were calculated after 1 hour of sliding and at the end of each test (7 h). The obtained values decrease in passing from short to long tests, and they are all coherent with a mild wear regime [21, 36]. The corresponding percent variation in the wear rate, η, was calculated as:

$$\eta = \left(K_a^{1h} - K_a^{7h}\right)/K_a^{1h}$$

where K_a^{1h} and K_a^{7h} are the specific wear coefficients after 1 h and 7 h of sliding, respectively. The negative values indicate, as expected, a reduction in the wear rate after the initial transient, compatible with the formation of more stable and protective friction layers after sufficiently long time periods, when steady state friction and wear conditions have been reached.

3.2 ANALYSIS OF WORN SURFACES

PRIMARY PLATEAUS

Fig.4 shows the worn surfaces of the friction materials (the pins) at the end of the PoD tests. Primary plateaus, made of metal fibers, and secondary plateaus, made of compacted wear particles, are clearly visible. On the *OM* pin's surface, the primary plateaus are mainly constituited by copper fibers. In the other two materials they are made by steel fibers only. Occasionally, some coarser particles also contribute to the formation of primary plateaus.

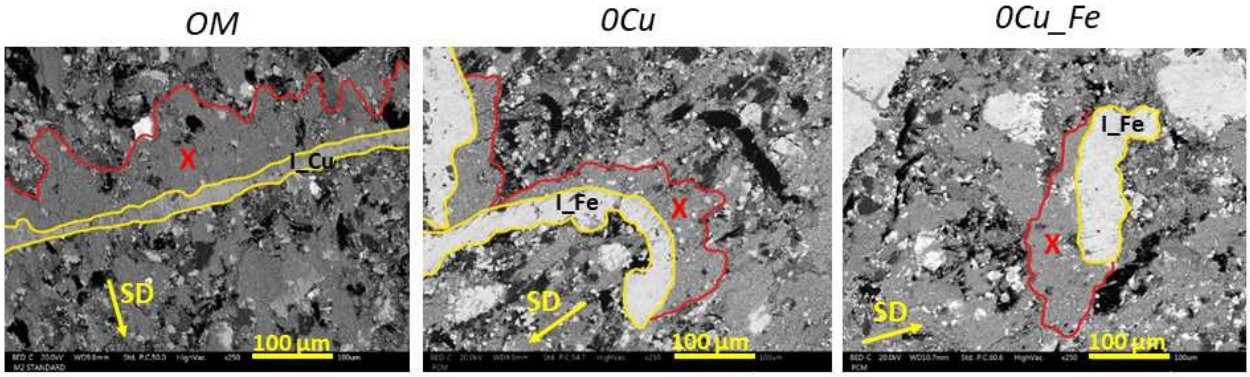

Fig.4 *SEM images of sliding surface of OM, 0Cu and 0Cu_Fe; the friction layers formed by the primary plateaus (metal fibers) and the secondary plateaus (compacted wear particles) can be observed. Legend: SD= sliding direction during pin-on-disc tests, l_Fe: primary plateaus made of steel fibers; l_Cu primary plateaus made of copper fibers, X secondary plateau.*

Fig.5 displays the pin worn surfaces at the end of the tests and at lower magnification. The metallic fibers protruding from the surface and forming the primary plateaus are visible in white. Image analysis was used for determining the extension of the primary plateaus. In the processed images the red colour represents the metal fibers. The extension of the primary plateaus was then obtained. It can be seen that the percent extension of the primary plateaus correlations with the total content of metal fibers that is around 20% in material *OM* and *0Cu_Fe* and approximately 5% in material *0Cu* that only contains the steel fibers already present in the Original Mix (*OM* sample).

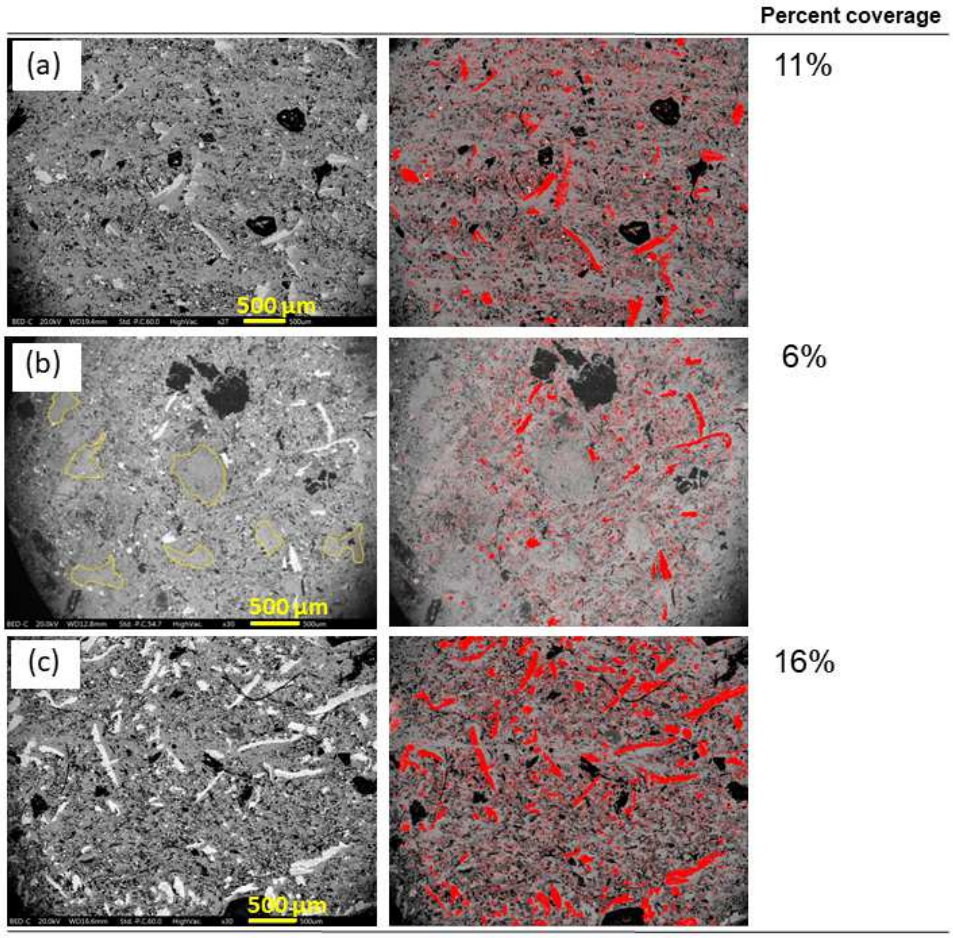

Fig.5 *Low magnification SEM images of the pin surface after PoD tests (7h): (a) OM, (b) 0Cu and (c) 0Cu_Fe. For each image the surface percentage of the primary plateaus (coverage factor) was estimated by image analysis. In 0Cu material (b) are present large secondary plateaus (marked in yellow) not supported by primary plateaus.*

SECONDARY PLATEAUS

In Fig.6, the planar view of the secondary plateaus of the three friction materials is shown after 1 h of sliding. Plateaus in the *0Cu* sample appear more fragmented and unrefined than those visible on the *OM* and *0Cu_Fe* sample surfaces. Moreover due to the low concentration of metallic fibers (6% see Fig.5b), the secondary plateaus on the surface of the sample *0Cu* appear often not supported by any primary plateaus (marked in yellow in Fig.5b). This type of secondary plateaus has been already reported in the literature and classified as “Type II” [5], with reference to NAO friction materials, being “Type I” the secondary plateaus that form with the support of primary plateaus.

For each friction material, three different SEM fields of view were considered for estimating the plateaus area and crack length (Fig. 6, samples PoD tested for 1 h). Plateaus were randomly selected and the SEM magnification was kept the same throughout the measurements. The measured lengths

of the cracks on the plateau were added up and then normalized to the plateau surface area, to estimate the crack surface density, expressed in μm/μm^2 and relevant standard deviation (Table 4). These results confirm that copper-free samples, *0Cu* and *0Cu_Fe*, after 1h testing, exhibit significantly more cracked plateaus, in comparison to the *OM* material. Interestingly, as shown by Fig.6, in all cases only a few small cracks were detected on the secondary plateaus at the end of the tests, i.e., after 7 h of sliding.

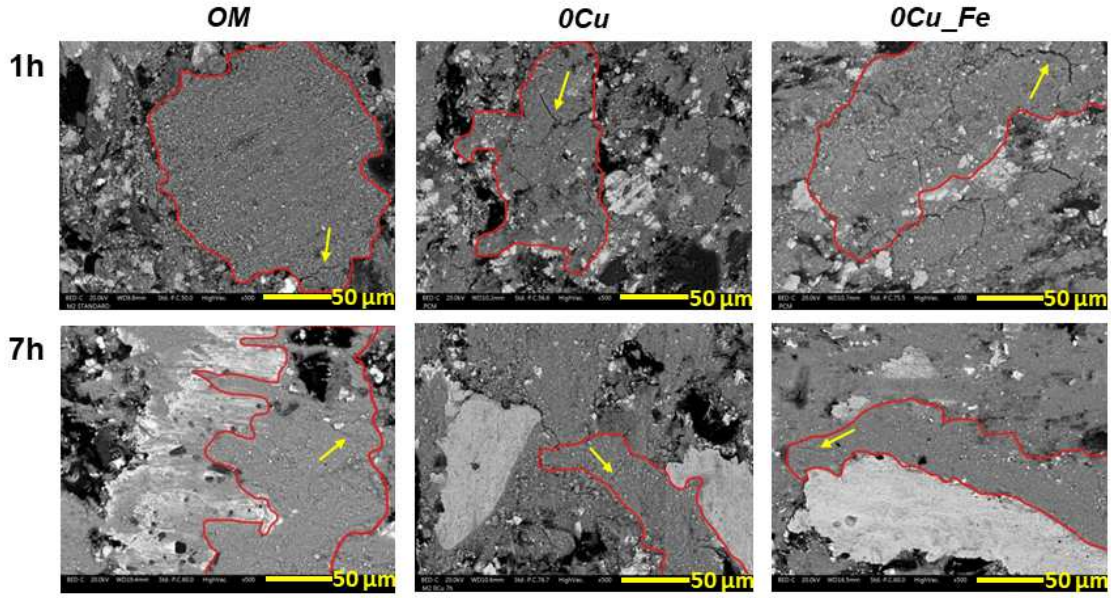

Fig.6 *SEM images of the plateaus in the samples OM, 0Cu and 0Cu_Fe wear tested at 1h and 7h. Secondary plateaus are marked. Cracks (arrowed) are visible in 1h tests for 0Cu and 0Cu_Fe samples. After 7h of tests, the cracks nearly disappear from 0Cu_Fe samples.*

Cracks on plateaus (μm/ μm^2)	***OM***	***0Cu***	***0Cu_Fe***
Mean value	0.0003	0.017	0.016
Standard deviation	0.0006	0.002	0.005

Table 4 *Surface density of the cracks observed in the secondary plateaus after tests carried out for 1h.*

Fig.7 shows the results of the image analysis, from which the extension of the primary and secondary plateaus after 1 h and 7 h of sliding in the case of material *0Cu_Fe* can be inferred. It turns out that the size of the primary and secondary plateaus does not change significantly in going from 1 h to 7 h of testing, proving that the plateaus reached a dynamic equilibrium at the end of short test already. The total extension of the friction layer (primary + secondary plateaus, figure 7) is in between 50-60% of the total surface area of the pin, in a good agreement with other experimental data [37]. Similar results

were obtained for the other two materials with some differences though. In case of material *OM*, the extension of the secondary plateaus is somewhat lower than in *0Cu_Fe*: 34% after 1 h of sliding and 39% after 7 h. However, their degree of compaction is very similar, as revealed by the presence of very dense red areas close to the primary plateaus. In case of material *0Cu*, the extension of the plateaus is slightly larger, being 40% after 1 h and 42% after 7 h.

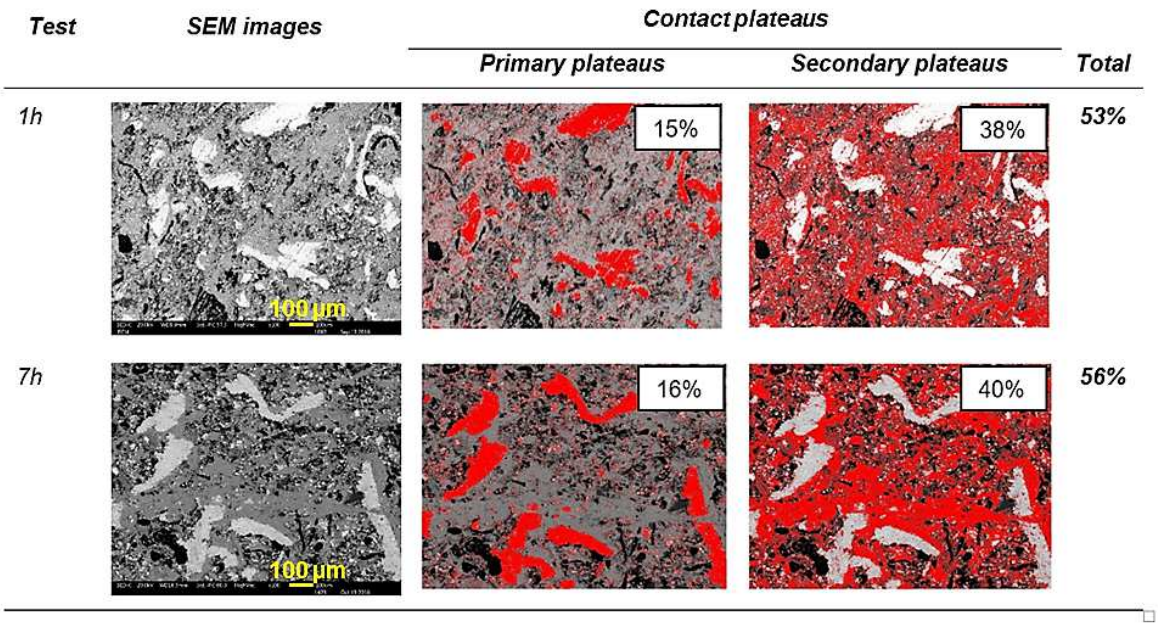

Fig.7 *The coverage factor of the friction layer was estimated for short (1h) and long (7h) tests by image analysis for the 0Cu_Fe material. SEM pictures and their image analysis re-elaboration. The TOTAL coverage factor was calculated summing-up the extension of primary and secondary plateaus.*

As an example, Fig. 8 shows a cross section of a secondary plateau close to a steel fiber for the material *0Cu_Fe, PoD tested for 7 h*. The plateau results from the compaction of micrometric particles. This is a peculiar characteristic of the secondary plateaus of all the investigated materials. Extensive EDXS analyses were carried out to evaluate the composition of the plateaus. The results are shown in Fig.9. In general, all elements present in the friction materials were detected, with the addition of a quite large amount of iron, showing that wear fragments from the counterface disc also enter into the secondary plateaus. The micrometric particles in the secondary plateaus are mainly made of iron oxides, zirconium oxide, potassium titanate, and other minor constituents originating from the wear of the friction material and couterface disc. As expected, the friction layer that forms on the material *OM* surface is rich in copper. It is also observed that copper content in *OM* increases in passing from the plateaus formed after 1 h of sliding to the plateau present on the worn surface at the end of the test (7 h). Iron also shows a different content in the secondary plateaus after 1 h of sliding and the end of the

test in the material *0Cu*. In fact, the iron content after 1 h is quite low, and it increases up to 30% at the end of the test.

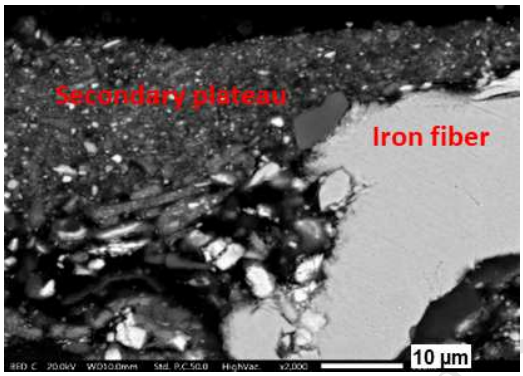

Fig.8 *SEM micrograph of the cross section of a secondary plateau close to a steel fiber - material 0Cu_Fe PoD testes for 7 h.*

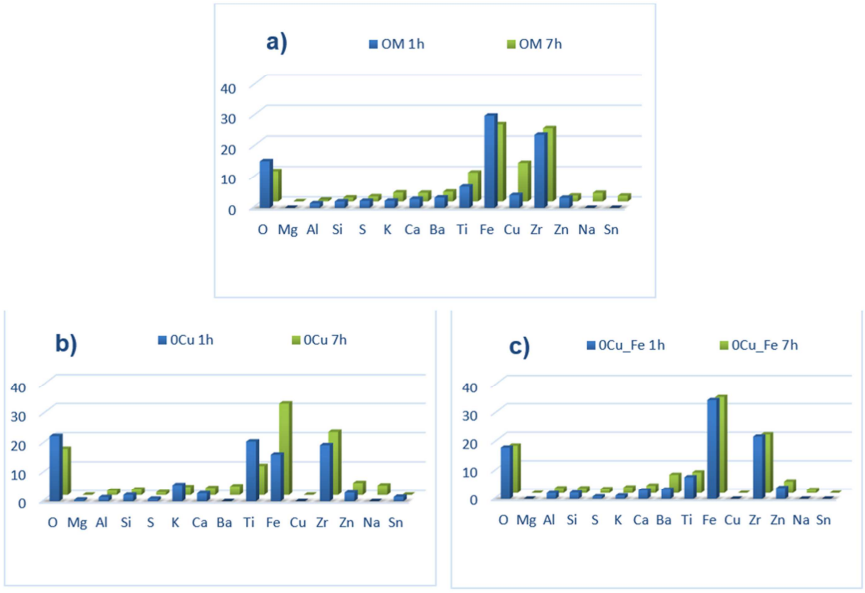

Fig.9 *EDXS data acquired on the secondary plateaus for OM (a), 0Cu (b) and 0Cu_Fe (c) referring to 1h (blue) and 7h (green) tests.*

4. DISCUSSION

The characteristics of the friction layer that forms during PoD sliding between the mating surfaces determine the friction and wear behavior of the materials under study [38-40]. In the following, we will first focus the discussion on the reference *OM* material, and then we will consider the effect of the removal of copper fibers (material *0Cu*) and their substitution with the same amount of steel fibers (material *0Cu_Fe*).

The results concerning the dry sliding behavior of the *OM* material substantially confirm what was found in previous investigations [15, 21]. Almost all elements present in the friction material are found in the secondary plateaus including iron (see Fig. 9a). This shows that such plateaus result from the compaction of small particles of wear debris from the friction material, including phase like: ZrO_2, $ZrSiO_4$ and K_2TiO_3 ; and iron oxides originating, to a large extent, from the tribo-oxidative wear of the cast iron counterface disc [17, 41]. Fig. 9a also shows that copper is present in the secondary plateaus that form on the *OM* pins, and its amount increases with the sliding time, i.e., in passing from short test to long test.

Copper is a soft metal and it is acknowledged to have an important role in the formation of well compacted secondary plateaus [14,15]. Copper nano-particles, produced by plastic deformation of the fibers, enter the secondary plateaus and help to increase their hardness and stability [11]. The SEM images in Fig. 6 show the beneficial effect of copper in reducing the cracks in the secondary plateaus of *OM*.

As regards iron in the secondary plateaus (Fig.9), in the *OM* material its concentration decreases from the short test to long test (steady-state conditions), whereas in the *0Cu_Fe* material it remains substantially constant all through the wear tests. Iron reaches its highest level in the steady-state conditions in the *0Cu* material.

During the early stage (1h) of the sliding process, metal fibers contribute to the tribo-oxidative wearing out of the disc. Steel fibers are more aggressive against the disc since they are harder than copper. After the early stage, a friction layer forms on the disc surface and on the pad surface. These layers are rich in iron oxides, which reduce the abrasive behavior [42].

In the steady-state conditions, the wearing out of the metal fibers becomes almost negligible, whereas their role as primary plateaus acquires a major importance. Both iron and copper fibers give support to the formation of the secondary plateaus and they resist against the local high temperature and the shear stresses.

As a matter of fact, the percent variation of the specific wear coefficient (Ƞ), is about the same for *OM* and *0Cu_Fe* (-50% and -55%, respectively), and lower for the material *0Cu* (-33%).

For all friction materials, specific wear coefficient is higher after 1 h test then at the end of the test (see Table 3). This is most likely due to a lower compaction of the secondary plateaus after a 1h test. The comparison with the behavior of the *0Cu* material allows us to get additional information on this point. The extension of the primary plateaus on the worn surface of materials is correlated with the total content of metallic fibers. *0Cu* presents approximately 6% of steel fibers on the worn surface (~5% of steel fibers are already present in the Original Mix). The extension of primary plateaus on material *OM* is greater, 11%, i.e., much less than the total amount of metallic fibers (the total amount of metallic fibers are approximately 20%, made by 5% of steel fibers and 15% of copper fibers).

We were not able to quantitatively discriminate between the steel and copper fibers present as primary plateaus on the worn surface of material *OM*, but it is clear that some of the copper fibers underwent sliding wear and with the transfer of the wear particles into the secondary plateaus [21]. Moreover, some of the fibers acting as primary plateaus in the *OM* material tend to be partially covered by the secondary plateaus (see relevant planar view in Fig.6, after 7h PoD test – sample *OM*). This situation artificially reduces the primary plateaus that are detectable by image analysis. The reason for this behavior can be reasonably traced back to both the lower hardness of copper fibers with respect to steel fibers and to the elevated surface energy of the ultra-fine grained particles in the secondary plateaus. This affinity to the metallic surface of the primary plateaus is enhanced further by the presence of metallic copper, coming from the wearing out of powders and fibers, as mentioned before, present in the *OM* friction material.

The *0Cu* material shows quite a different tribological behavior in comparison to the *OM* material: in the steady-state condition, wear rate is higher and friction coefficient is lower. As a consequence of the removal of copper fibers from the composition, the extension of the primary plateaus is reduced from 11% to 6%. As concerns the secondary plateaus, the *0Cu* material exhibits the prevailing presence of the so-called “Type II” plateaus [5], i.e., those forming without the support of primary plateaus. These structures, that cover large areas of the pin surface, reduce the friction coefficient, as actually observed in the present study (Table 3).

Coherently with the low fraction of metallic fibers, a limited fraction of “Type I” secondary plateaus is also observed in the *0Cu* material. This type of secondary plateaus is the standard for the other two materials (*OM* and *0Cu_Fe*).In the material *0Cu*, the density of cracks appearing in secondary contact plateaus is particularly high after 1 h sliding, i.e., when steady-state conditions are not yet achieved. The formation of cracks can be ascribed to the absence of copper. The presence of similar cracks in secondary plateaus has been reported already by Bettge et al. [43]. In that case, the pads considered for the frictional studies did not contain copper. At the end of the PoD tests, a few cracks only were detected in the secondary plateaus (Fig.6) in all materials, showing that, during steady-state sliding conditions, a better compaction of the plateaus was reached. Correspondingly, the specific wear coefficient was found to decrease in passing from running-in to steady state (Table 3).

Material *0Cu_Fe* displays a friction and wear behavior that is in a way intermediate in between the reference material *OM* and material *0Cu*. The friction coefficient is higher than that of material *0Cu* and only slightly lower than material *OM*. The higher friction coefficient, with respect to *0Cu*, can be clearly attributed to the increase in the extension of primary plateaus from 6 % (in material *0Cu*) to 16% (Figure 5). In this material, primary plateaus on the top surface take up a larger area then in the *OM* material (11%). All the primary plateaus on the *0Cu_Fe* material are made of steel fibers and the increase in the adhesive interactions between the steel fibers in the friction material and the cast iron

counterface disc increase the friction coefficient [28]. The absence of copper reduces the compactness of the secondary plateaus and this is coherent with the presence of cracks in the plateaus after 1 h testing (Fig. 6). This is in agreement with the fact that the relevant specific wear rate evaluated after 1 h PoD test is slightly higher for the sample *0Cu_Fe* than that displayed by material *0Cu*. However, during steady-state wear regime the specific wear rate decreases and becomes lower than in material *0Cu*, thanks to the formation, favored by the large number of primary plateaus available, of well compacted secondary plateaus with a fine granulometry.

In Fig. 10, the specific wear rates of the investigated friction materials are plotted as a function of the steady-state friction coefficients. Quite interestingly, the K_a-values are inversely proportional to the μ_{ss}-values. In general, when comparing different friction materials, wear rate increases with friction coefficient, and this is typically due to the presence of abrasives in the friction material compositions, that induce an increase in both friction coefficient and wear rate [1]. However, in the materials considered in the present study, no evidence of abrasive interactions was detected and the different behaviour of the tested materials is then mainly due to differences in the characteristics of the friction layers (primary and secondary plateaus). As we have seen, an increase in the extension and compactness of the friction layer induces a decrease in wear rate and a correspondingly an increase in the friction coefficient because of the increased intensity of the adhesive interactions.

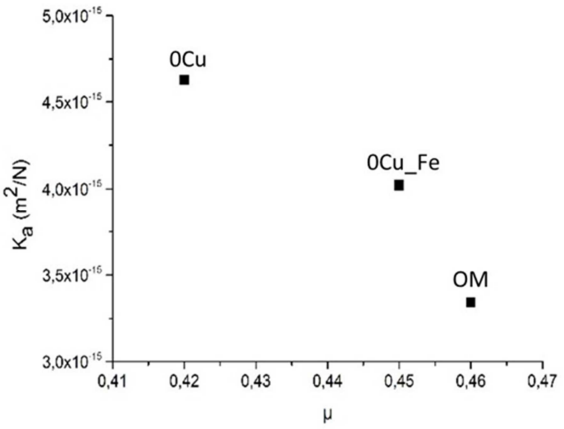

***Fig. 10**. Experimental relationship between the specific wear coefficient (K_a) and the mean friction coefficients attained during the steady-state regime.*

5. CONCLUSIONS

From a reference friction material (*OM*), copper fibers and powder were fully eliminated to produce other two materials; the *0Cu* material, without any replacement; and the *0Cu_Fe* material in which the copper fibers (15% wt.) quota was replaced by steel fibers. All three materials have been wear tested against cast iron using a PoD test rig. The main conclusions are:

- The friction coefficient is indeed dependent on the compactness and stability of the friction layer. The best conditions are observed in *OM* and *0Cu_Fe* materials with well distributed metallic fibers, that offer a solid support to the trapping and densification of wear debris. The secondary plateaus that form in this way are compact, adherent and comparatively tougher that those forming on the *0Cu* material, in which are observed large secondary plateaus, that form without the support of any fiber (primary plateaus).
- The material *0Cu* exhibits the highest wear and the lowest friction coefficient. Material *0Cu_Fe* have higher wear rates in the short-term tests, when the friction layer is not yet well consolidated.
- However, when the steady-state is reached, after the formation of a stable friction layer, the wearing out of the steel fibers becomes almost negligible, whereas acquires more importance their role as primary plateaus. At this stage, the steel fibers act as the copper fibers and form the primary plateaus.
- In the material *0Cu* and *0Cu_Fe* when steady-state conditions are not yet achieved (1 h test), many cracks are present on the secondary plateaus, as compared to *OM* material. The formation of these cracks can be mostly attributed to the absence of copper. During the steady-state, most of the cracks disappeared.
- A promising route to follow, heading towards copper-free friction materials, seems to be the attainment of the right balance between primary and secondary plateaus that together contribute to form a solid and tough friction layer.

This conclusion is correct for mild wear and low contact temperature conditions. However, copper is known to be very effective with regard to friction and wear also in the case of sliding in severe conditions, i.e., when the contact temperature is high, typically in excess of 250-300°C [11]. A future investigation is therefore necessary to understand the comparitive behaviour of the material with copper or steel fibers on the sliding behaviour in severe wear conditions.

ACKNOWLEDGEMENTS

The Authors would like to thank Guido Perricone, Brembo SpA, for his enthusiastic support to the research and useful discussions.

REFERENCES

[1] Chan D, Stachowiak GW. Review of automotive brake friction materials. J. Automobile Engineering, Proc. Instn. Mech. Engrs 2004; vol. 218 (Part D):953–966.

[2] Xiao X, Yin Y, Bao J, Lu L, Feng X. Review on the friction and wear of brake materials. Adv Mech Eng 2016;8(5):1-10.

[3] Eriksson M, Jacobson S. Tribological surfaces of organic brake pads. Tribol Int 2000;33:817–827.

[4] Österle W, Urban I. Third body formation on brake pads and rotors. Tribol Int 2006;39:401-408.

[5] Neis PD, Ferreira NF, Fekete G, Matozo LT, Masotti D. Towards a better understanding of the structures existing on the surface of brake pads. Tribol Int 2017;105:135-147.

[6] Denier van der Gon HAC, Hulskotte JHJ, Visschedijk AJH, Schaap M. A revised estimate of copper emissions from road transport in UNECE-Europe and its impact on predicted copper concentrations. Atmos Environ 2007;41(38):8697-8710.

[7] Bijwe J, Kumar M, Gurunath p V, Desplanques Y, Degallaix G. Optimization of brass contents for best combination of tribo-performance and thermal conductivity of non-asbestos organic (NAO) friction composites. Wear 2008;265:699–712.

[8] Lee PW, Filip P. Friction and wear of Cu-free and Sb-free environmental friendly automotive brake materials. Wear 2013;302:1404-1413.

[9] Straffelini G, Ciudin R, Ciotti A, Gialanella S. Present knowledge and perspectives on the role of copper in brake materials and related environmental issues: A critical assessment. Environmental Pollution 2015;207:211-219.

[10] Bode K, Ostermeyer GP. A comprehensive approach for the simulation of heat and heat-induced phenomena in friction materials. Wear 2014;311:47–56.

[11] Österle W, Prietzel C, Kloß H, Dmitriev AI. On the role of copper in brake friction materials. Tribol Int 2010;43:2317–2326.

[12] Österle W, Griepentrog M, Gross T, Urban I. Chemical and microstructural changes induced by friction and wear of brakes. Wear 2001;251:1469–1476.

[13] Eriksson M, Bergmann F, Jacobson S. On the nature of tribological contact in automotive brakes. Wear 2002;252:26–36.

[14] Kumar M, Bijwe J. Non-asbestos organic friction composites: role of copper; its shape and amount. Wear 2011;270:269–280.

[15] Menapace C, Leonardi M, Perricone G, Bortolotti M, Straffelini G, Gialanella S. Pin-on-disc study of brake friction materials with ball-milled nanostructured components. Materials and Design 2017;115:287–298.

[16] Österle W, Prietzel C, Dmitriev AI. Investigation of surface film nanostructure and assessment of its impact on friction force stabilization during automotive braking. Int J Mater Res 2010;101:1–7.

[17] Verma PC, Menapace L, Bonfanti A, Ciudin R, Gialanella S, Straffelini S. Braking pad-disc system: wear mechanisms and formation of wear fragments. Wear 2015;322- 323:251-258.

[18] Eriksson M, Bergman F, Jacobson S. Surface characterization of brake pads after running under silent and squealing conditions. Wear 1999;232:163–167.

[19] Ouyang H, Nack W, Yuan Y, Chen F. Contact FE model to simulate disc brake squeal: a review. Int J Vehicle Noise and Vibration 2005;Vol.1 Nos.3/4.

[20] Kukutschova J, Roubíceka V, Malachovab K, Pavlíckovab Z, Holusab R, Kubackovac J, Mickac V, Crimmond DM, Filip P. Wear mechanism in automotive brake materials, wear debris and its potential environmental impact. Wear 2009;267:807-817.

[21] Verma PC, Ciudin R, Bonfanti A, Aswath P, Straffelini G, Gialanella S. Role of the friction layer in the high-temperature pin-on-disc study of a brake material. Wear 2016;346-347:56–65.

[22] Sharma S, Bijwe J, Kumar M. Comparison between nano- and micro-sized copper particles as fillers in NAO friction materials. Nanomater Nanotechnol 2013;Vol.3:Art.12.

[23] Aranganathan N, Bijwe J. Special grade of graphite in NAO friction materials for possible replacement of copper. Wear 2015;330-331:515–523.

[24] Panda JN, Bijwe J, Pandey RK. Role of treatment to graphite particles to increase the thermal conductivity in controlling tribo-performance of polymer composites. Wear 2016;360-361:87–96.

[25] Aranganathan N, Bijwen J. Development of copper-free eco-friendly brake-friction material using novel ingredients. Wear 2016;352-353:79–91.

[26] Sanders PG, Xu N, Dalka TM, Maricq M. Airborne brake wear debris, size distributions, composition, and a comparison of dynamometer and vehicle tests. Environ Sci Technol 2003;37:4060-4069.

[27] Huang X, Moir RD, Tanzi RE, Bush AI, Rogers JT. Redox-active metals, oxidative stress, and Alzheimer's disease pathology. Annals of the New York Academy of Sciences 2004;1012:153–163.

[28] Kumar M, Bijwe J. Optimized selection of metallic fillers for best combination of performance properties of friction materials : A comprehensive study. Wear 2013;303:569-583.

[29] Kchaou M, Mat Lazim AR, Abu Bakar AR, Fajoui J, Elleuch J, Jacquemin F. Effects of steel fibers and surface roughness on squealing behavior of friction materials. Trans Indian Inst Met 2016; DOI 10.1007/s12666-015-0688-4.

[30] Jang H, Ko K, Kim SJ, Basch RH, Fash JW. The effect of metal fibers on the friction performance of automotive brake friction materials. Wear 2004;256:406-414.

[31] Flores A, Lopez M, Avalos A, Gonzalez G, Garcìa O. The influence of steel fiber contents in the formation of tribofilms. Proceeding of EUROBRAKE 2016; Milan 13-15 June 2016, MDS-028.

[32] Park SB, Cho KH, Jung S, Jang H. Tribological properties of brake friction materials with steel fibers. Metals Mater Int 2009;15:27-32.

[33] Straffelini G, Verma PC, Metinoz I, Ciudin R, Perricone G, Gialanella S. Wear behavior of a low metallic friction material dry sliding against a cast iron disc: Role of the heat-treatment of the disc. Wear 2016;348-349:10–16.

[34] Kchaou M, Sellami A, Elleuch R, Singh H. Friction characteristics of brake friction material under different braking conditions. Materials and Design 2013;52:533-540.

[35] Hutchings M. Friction and Wear of Engineering Materials. London: Edward Arnold; 1992.

[36] Straffelini G. Friction and Wear: Methodologies for Design and Control. Springer; 2015.

[37] Yoon SW, Shin MW, Lee WG, Jang H. Effect of surface contact conditions on the stick–slip behavior of brake friction material. Wear 2012;294-295:305-312.

[38] Barros LY, Neis PD, Ferreira NF, Pavlak RP, Masotti D, Matozo LT, Sukumaranc J, De Baets P, Andó M. Morphological analysis of pad-disc system during braking operations. Wear 2016;352-353:112-121.

[39] Filip P, Weiss Z, Rafaja D. On friction layer formation in polymer matrix composite materials for brake applications. Wear 2002;252:189-198.

[40] Xu X, Lu X, Qin Z, Yang D. The study of friction layer and tribological property of PI–matrix composites. Industrial Lubrication and Tribology 2017;69:267-275.

[41] Straffelini G, Maines L. The relationship between wear of semimetallic friction materials and pearlitic cast iron in dry sliding. Wear 2013;307:75-80.

[42] Alemani M, Gialanella S, Straffelini G, Ciudin R, Olofsson U, Perricone G, Metinoz I. Dry sliding of a low steel friction material against cast iron at different loads: Characterization of the friction layer and wear debris. Wear 2017;376-377:1450-1459.

[43] Bettge D, J.Starcevic J. Topographic properties of the contact zones of wear surfaces in disc brakes. Wear 2003;254:195-202.

Highlights

- Steel fibers have been studied with the aim of develop copper-free friction materials.
- Pin-on-disc tests were carried out comparing three innovative friction materials.
- Balanced primary and secondary plateaus are the key for a stable friction layer.